Simple theory of electronic-structure calculations for amorphous transition-metal alloys

Y. Kakehashi
Hokkaido Institute of Technology, Maeda, Teine-ku, Sapporo 006, Japan

H. Tanaka
IBM Research, Tokyo Research Laboratory, IBM Japan Ltd. 1623-14, Shimotsuruma, Yamato, Kanagawa 242, Japan

M. Yu
Hokkaido Institute of Technology, Maeda, Teine-ku, Sapporo 006, Japan
(Received 15 September 1992; revised manuscript received 30 November 1992)

A theory of electronic-structure calculations for amorphous alloys is presented on the basis of a geometrical-mean model for amorphous structures and transfer integrals. It greatly simplifies the numerical calculations by constructing the electronic structures of amorphous alloys from those of constituent amorphous pure metals, and describes the local environment effects by introducing the average coordination numbers z_α^* and atomic short-range-order parameters τ_α for each type of atom α. It is demonstrated, by comparing the numerical results with those obtained from first-principles, that the theory reasonably describes the electronic structure of amorphous transition-metal alloys. In particular, it is shown that the difference in z_α^*, which is caused by constituent atoms with different atomic sizes, stabilizes the ferromagnetism in amorphous $Fe_{65}Zr_{35}$ and Co_2Y alloys since it builds up a high-energy peak around the Fermi level.

I. INTRODUCTION

Amorphous transition-metal alloys often show a drastic change of magnetism because of their structural and configurational disorders. For example, Fe-rich amorphous alloys show a rapid decrease of magnetization with increasing Fe concentration, and fall into the spin-glass state after complete disappearance of ferromagnetism.[1–4] The magnetic moments and Curie temperatures in Co-rich Co-Y amorphous alloys are well known to be enhanced as compared with those in their Laves-phase crystalline counterparts.[5] Some Heusler alloys such as the Cu_2MnAl alloy show a remarkable change from the strong ferromagnet to the spin glass with the formation of amorphous structure.[6]

The electronic-structure calculations of amorphous alloys provide us with a base to understand the physics for drastic changes of magnetism mentioned above. The purpose of this paper is to propose a geometrical-mean (GM) model for a semiquantitative calculation of the electronic structure in amorphous transition-metal alloys and to develop an analytical theory that drastically simplifies the numerical calculations of densities of states (DOS's) and Green's functions for amorphous alloys.

Needless to say, theories of electronic-structure calculations for amorphous alloys have been developed extensively in the last decade.[7–18] In particular, Fujiwara[10] developed a first-principles method by combining the tight-binding linear-muffin-tin-orbital (LMTO) method[19] with the recursion method[20] for electronic-structure calculations. The supercell approach,[11,12,15,18] in which an amorphous alloy is simulated by an amorphous "compound" with a large number of atoms in a unit cell, also became reliable with the development of supercomputers.

Although these methods provide us with accurate electronic structures for amorphous alloys, they have some disadvantages in the actual applications. First, the calculations based on the first-principles methods are too laborious, so that they are not suitable for the systematic investigations for a large number of amorphous alloys and for the applications to more complicated problems such as the finite-temperature magnetism, in which we have to calculate one-electron Green's functions in various random-exchange fields.[21–24]

Second, the amorphous structures used in the first-principles electronic-structure calculations are generated on computers usually by means of the relaxed dense random packing of hard spheres (DRPHS) model[10,17] so that the calculated pair-distribution functions agree with the experimental data. The data, however, are often missing in the literature, so that it is not easy to perform the systematic investigations.

Third, the first-principles methods are nonanalytic and treat all the information on amorphous structures as the input data. Thus, it is not easy to find from the numerical results the basic parameters controlling the electronic structure of amorphous alloys. The present theory complements these disadvantages of the first-principles methods and leads to qualitative or semiquantitative understanding of the electronic structures in amorphous alloys.

In the following section, we introduce the GM model, which reduces the off-diagonal configurational disorder in a tight-binding Hamiltonian into a diagonal disorder. The validity of the model will be discussed there. In Sec. III, we develop a single-site theory on the basis of the GM model. Numerical examples will be presented for $Cu_{35}Zr_{65}$ and $Fe_{65}Zr_{35}$ amorphous alloys. The theory is

improved using a Bethe-type approximation in Sec. IV to take into account the local environment effects (LEE's) on the electronic structures in amorphous alloys. We introduced there average coordination numbers z_α^* for atom α as well as atomic short-range order (ASRO) parameters τ_α. The parameters z_α^* describe the atomic-size effects, which are characteristic of amorphous 3*d*-4*d*, 3*d*-5*d*, and 3*d*-rare-earth alloys. We will demonstrate in Sec. V that the parameters z_α^*, as well as τ_α, change the shape of the DOS drastically. In particular, we point out an important role of the atomic-size difference on the stability of ferromagnetism in amorphous $Fe_{65}Zr_{35}$ and Co_2Y alloys. The last section, VI, is devoted to a summary and discussions on possible applications.

II. GEOMETRICAL-MEAN MODEL FOR ELECTRONIC-STRUCTURE CALCULATIONS

We consider a binary (*A*-*B*) amorphous alloys described by a simple tight-binding Hamiltonian as follows:

$$H=\sum_{i,\sigma}\epsilon_i n_{i\sigma}+\sum_{i,j,\sigma}t'_{ij}a^\dagger_{i\sigma}a_{j\sigma}\ . \tag{1}$$

Here ϵ_i and t'_{ij} are the atomic level on site i and the transfer integral between sites i and j, respectively. $a^\dagger_{i\sigma}(a_{i\sigma})$ denotes the creation (annihilation) operator for an electron with spin σ on site i, and $n_{i\sigma}=a^\dagger_{i\sigma}a_{i\sigma}$ denotes the electron number operator.

The electronic structure for the Hamiltonian (1) is calculated from a one-electron Green's function defined by

$$G_{ij}=[(\omega+i\delta-\epsilon-t')^{-1}]_{ij}\ . \tag{2}$$

Here the matrices are defined by $(\epsilon)_{ij}=\epsilon_i\delta_{ij}$ and $(t')_{ij}=t'_{ij}$, respectively. The spin index σ is omitted for brevity. δ in Eq. (2) is an infinitesimal positive number.

The amorphous alloys possess the configurational and structural disorders; atomic levels $\{\epsilon_i\}$ and transfer integrals $\{t'_{ij}\}$ change randomly according to the atomic configuration $\{\gamma_i\}$ and the interatomic distance $\{R_{ij}\}$, where γ_i denotes a type of atom on site i and R_{ij} is the interatomic distance between sites i and j.

It should be noted that the theoretical treatment of the off-diagonal disorder associated with t'_{ij} is more difficult than that of the diagonal disorder in ϵ_i. To simplify the calculations for the former, we introduce a geometrical-mean (GM) model with the following properties. (i) The transfer integral $t'_{ij}=t^{\alpha\gamma}(R_{ij})$ is given by a geometrical mean: $t^{\alpha\gamma}(R_{ij})=[t^{\alpha\alpha}(R_{ij})t^{\gamma\gamma}(R_{ij})]^{1/2}$. Here α (γ) denotes the type of atom on site i (j). Note that the transfer integral $t^{\alpha\alpha}(R_{ij})$ depends on α and γ via R_{ij} because of the difference in atomic size. (ii) The interatomic distance R_{ij} is dominated by the types of atoms α on site i and γ on site j, and is given by a geometrical mean: $R_{ij}^{\alpha\gamma}=(R_{ij}^{\alpha\alpha}R_{ij}^{\gamma\gamma})^{1/2}$. (iii) The transfer integrals follow the same power law with respect to the interatomic distance: $t'_{ij}\propto R_{ij}^{-\kappa}$, κ being independent of the type of atoms. (iv) The amorphous pure metals *A* and *B* have the same structure: $R_{ij}^{AA}=\Lambda R_{ij}^{BB}$, where Λ is a proportionality constant independent of sites i and j. In other words, we may assume that the amorphous *B* metal, which was constructed so as to be similar to the structure of amorphous *A* metal, gives the same electronic structure as in the *real* amorphous *B* metal after taking the structural average.

The first assumption was proposed in the substitutional alloys,[25] and it is recognized as a reasonable approximation in transition-metal alloys. The second assumption is expected to hold true approximately for the nearest-neighbor interatomic distance, since the amorphous alloys have a structure similar to the dense random packing of hard spheres (DRPHS) model. We have compared R_{ij}^{AB} with $(R_{ij}^{AA}R_{ij}^{BB})^{1/2}$ in amorphous Fe-La (Ref. 26) and Cu-Zr (Ref. 27) alloys and have verified that the second assumption holds true within a few percent error as shown in Figs. 1 and 2. Although the second assumption is not expected generally for further distant pairs, we emphasize that the nearest-neighbor transfer integrals are dominant in the DRPHS-like structures and thus determine the main part of the electronic structure. The power-law relation in the third assumption is verified in the band theory, and the same exponent $\kappa\approx 5$ is expected for the transition-metal–transition-metal alloys.[19,28] The fourth assumption is based on the fact that the essential part of a large number of experimental pair-distribution functions in metallic alloys is explained by a simple DRPHS-like model independently of their bonding nature.[29,30]

We obtain from assumption (i) the following relation:

$$t'_{ij}=r_\alpha^{(c)*}t_{ij}r_\gamma^{(c)}\ . \tag{3}$$

Here we can choose t_{ij}, for example, as $t_{ij}=t^{BB}(R_{ij}^{\alpha\gamma})$. It should be noted that t_{ij} still depends on the types of

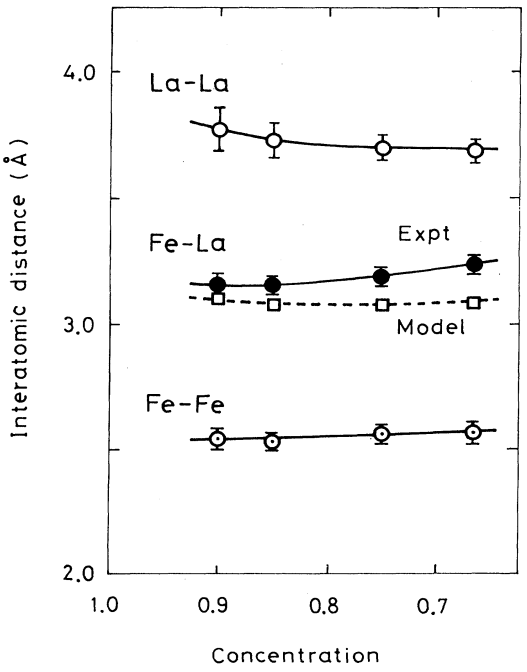

FIG. 1. Nearest-neigbor interatomic distances in amorphous Fe_cLa_{1-c} alloys (Ref. 27). Dashed curve shows Fe-La distance calculated from the geometrical-mean (GM) model.

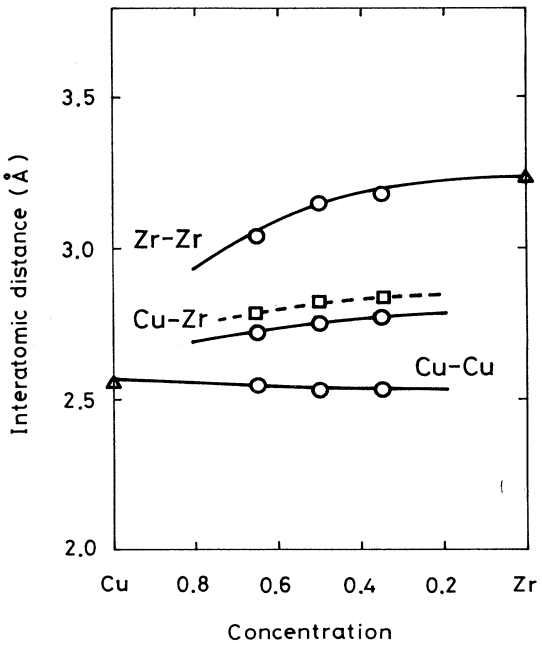

FIG. 2. The same as in Fig. 1, but for amorphous Cu_cZr_{1-c} alloys (Ref. 26).

atoms α and γ via $R_{ij}^{\alpha\gamma}$, but $r_\alpha^{(c)}$ only depends on the type of atom α because of assumption (iii):

$$r_\alpha^{(c)}=\left[\frac{t^{\alpha\alpha}(R_{ij}^{\alpha\gamma})}{t^{BB}(R_{ij}^{\alpha\gamma})}\right]^{1/2} . \tag{4}$$

Furthermore, we have following relation from assumptions (ii) and (iii):

$$t_{ij}=r_\alpha^{(s)*}\hat{t}_{ij}r_\gamma^{(s)} . \tag{5}$$

Here $\hat{t}_{ij}=t^{BB}(R_{ij}^{BB})$ does not depend on the atomic configuration any more. The factor $r_\alpha^{(s)}$ is defined by

$$r_\alpha^{(s)}=\left[\frac{t^{\alpha\alpha}(R_{ij}^{\alpha\alpha})}{t^{BB}(R_{ij}^{BB})}\right]^{1/2} , \tag{6}$$

and it is independent of sites i and j because of the assumption (iv).

From Eqs. (3) and (5) we obtain

$$t'_{ij}=t^{\alpha\gamma}(R_{ij}^{\alpha\gamma})=r_\alpha^{*}\hat{t}_{ij}r_\gamma , \tag{7}$$

$$r_\alpha=r_\alpha^{(s)}r_\alpha^{(c)}=\begin{cases} r_A & (\alpha=A) \\ 1 & (\alpha=B) \end{cases} . \tag{8}$$

The factor r_A is obtained from the second moments as follows:

$$\sum_j t^{AA}(R_{j0}^{AA})^2=|r_A|^4\sum_j t^{BB}(R_{j0}^{BB})^2 . \tag{9}$$

After taking the structural disorder, we obtain $|r_A|^2$ as follows:

$$|r_A|^2=\left[\frac{\mu_2(A)}{\mu_2(B)}\right]^{1/2} . \tag{10}$$

Here $\mu_2(\alpha)$ is the second moment for the average density of states (DOS) for amorphous pure metal α:

$$\mu_2(\alpha)=\int\epsilon^2[\rho_\alpha^0(\epsilon)]_s d\epsilon . \tag{11}$$

Here $[\ ]_s$ denotes the structural average.

By making use of the relation (7), the Green's function (2) is written as follows:

$$G_{ij}=\frac{1}{r_\alpha}[(\hat{L}^{-1}-\hat{t})^{-1}]_{ij}\frac{1}{r_\gamma^*} . \tag{12}$$

Here $(\hat{t})_{ij}\equiv\hat{t}_{ij}$ and the locator $\hat{L}$ is defined by

$$(\hat{L}^{-1})_{ij}=\hat{L}_i^{-1}\delta_{ij}=\frac{\omega+i\delta-\epsilon_i}{|r_\alpha|^2}\delta_{ij} . \tag{13}$$

Equation (12) shows that the off-diagonal disorder for atomic configuration in the transfer integrals has been transformed into a diagonal disorder in the locator $\hat{L}$. In other words, the system has been transformed into a substitutional alloy with random potentials on a network for amorphous pure metal, so that one can construct a theory using the methods developed in the substitutional alloys. In the following section, we present a single-site theory.

III. SINGLE-SITE APPROXIMATION

We adopt the locator expansion[25,31] as follows to treat the Green's function $\hat{G}_{ij}=r_\alpha G_{ij}r_\gamma^*$:

$$\begin{aligned}\hat{G}&=(\hat{L}^{-1}-\hat{t})^{-1}\\&=\hat{L}+\hat{L}\hat{t}\hat{L}+\hat{L}\hat{t}\hat{L}\hat{t}\hat{L}+\cdots .\end{aligned} \tag{14}$$

Taking the diagonal element of $\hat{G}$ at the origin, we have a relation,

$$\begin{aligned}\hat{G}_{00}&=\hat{L}_0+\hat{L}_0S_0(\hat{L}_0)\hat{L}_0+\cdots\\&=\frac{1}{\hat{L}_0^{-1}-S_0(\hat{L})} .\end{aligned} \tag{15}$$

Here $S_0(\hat{L})$ denotes the sum of all the paths in which an electron starts from site 0 and end at site 0 without returning to site 0 on the way.

In the single-site approximation (SSA), we replace the locators outside the origin with an energy-dependent effective locator $\mathcal{L}$:

$$[\hat{G}_{00}]_c=\frac{1}{\hat{L}_0^{-1}-S_0(\mathcal{L})} . \tag{16}$$

Here $[\ ]_c$ denotes the configurational average when the central atom is fixed. The self-energy is related to the Green's function with the effective locator as follows:

$$[(\mathcal{L}^{-1}-\hat{t})^{-1}]_{00}=\frac{1}{\mathcal{L}^{-1}-S_0(\mathcal{L})} . \tag{17}$$

We next replace $S_0(\mathcal{L})$ with an effective self-energy $\mathcal{S}_0$ when we take the structural average in Eqs. (16) and (17):

$$\left[\left[\hat{G}_{\alpha\alpha}\right]_c\right]_s=\frac{1}{\hat{L}_\alpha^{-1}-\mathcal{S}_0}\ , \tag{18}$$

$$F(\mathcal{L}^{-1})\equiv[((\mathcal{L}^{-1}-\hat{t})^{-1})_{00}]_s=\frac{1}{\mathcal{L}^{-1}-\mathcal{S}_0}\ . \tag{19}$$

Here $\hat{L}_\alpha$ denotes the locator for the type of atom α at the origin.

Eliminating the self-energy $\mathcal{S}_0$ from Eqs. (18) and (19), we obtain the expression for $[[G_{\alpha\alpha}]_c]_s=[[\hat{G}_{\alpha\alpha}]_c]_s/|r_\alpha|^2$ as follows:

$$[[G_{\alpha\alpha}]_c]_s=\frac{1}{|r_\alpha|^2}\frac{1}{\hat{L}_\alpha^{-1}-\mathcal{L}^{-1}+F(\mathcal{L}^{-1})^{-1}}\ . \tag{20}$$

The coherent Green's function $F(\mathcal{L}^{-1})$ is given by the local DOS $\rho^0(\epsilon)$ for the transfer integrals $\{\hat{t}_{ij}\}$ as follows:

$$F(\mathcal{L}^{-1})=\int\frac{[\rho^0(\epsilon)]_s d\epsilon}{\mathcal{L}^{-1}-\epsilon}\ . \tag{21}$$

The effective locator $\mathcal{L}$ is determined from the condition that the impurity Green's function (18) should be identical with the coherent Green's function (19) after taking the configurational average:

$$\sum_\alpha c_\alpha[\hat{L}_\alpha^{-1}-\mathcal{L}^{-1}+F(\mathcal{L}^{-1})^{-1}]^{-1}=F(\mathcal{L}^{-1})\ , \tag{22}$$

where c_α is the concentration of atom α. The above equation is well known as the coherent-potential-approximation (CPA) equation.[25]

The atomic levels $\{\epsilon_\alpha\}$ in the locators $\{\hat{L}_\alpha\}$ are determined to satisfy the local charge neutrality at each site:

$$n_\alpha=\int_{-\infty}^{0}d\omega\,\rho_\alpha(\omega)\ . \tag{23}$$

Here the energy ω is measured from the Fermi level. n_α is the electron number for pure metal α, and $\rho_\alpha(\omega)$ is the local DOS for atom α given by

$$\rho_\alpha(\epsilon)=-\frac{D}{\pi}\mathrm{Im}[[G_{\alpha\alpha}(\omega+i\delta)]_c]_s\ . \tag{24}$$

Here we introduced the number of degeneracy D ($D=5$ for transition metals) assuming D-fold equivalent bands for brevity.

According to Eq. (7), the shape of the DOS for amorphous pure metals defined by $\{t^{\alpha\alpha}(R_{ij}^{\alpha\alpha})\}$ is common to the constituent metals A and B. To describe the different shapes of DOS in both pure-metal limits (i.e., $c_\alpha=0$ and 1), as expected in $3d$-$4d$ and $3d$-$5d$ amorphous alloys, we consider the concentration dependence of the transfer integrals $\{\hat{t}_{ij}\}$, and adopt the common band model as follows:

$$\hat{t}_{ij}=\lambda\tilde{t}_{ij}=\lambda[c_A t_{ij}(A)+c_B t_{ij}(B)]\ . \tag{25}$$

Here $t_{ij}(\alpha)\equiv t^{\alpha\alpha}(R_{ij}^{\alpha\alpha},c_\alpha=1)$.

The coherent Green's function $F(\mathcal{L}^{-1})$ in the common band model may be obtained approximately by equating the self-energy $\mathcal{S}_0$ defined by Eq. (19) in which $\{\hat{t}_{ij}\}$ have been replaced by $\{\tilde{t}_{ij}\}$, with an average $c_A\mathcal{S}_0(A)+c_B\mathcal{S}_0(B)$, $\mathcal{S}_0(\alpha)$ being the self-energy for $\{t_{ij}(\alpha)\}$. The result is given by

$$F(\mathcal{L}^{-1})=[c_A F_A(\mathcal{L}^{-1})^{-1}+c_B F_B(\mathcal{L}^{-1})^{-1}]^{-1}\ , \tag{26}$$

$$F_\alpha(\mathcal{L}^{-1})=\int\frac{[\rho_\alpha^0(\epsilon)]_s d\epsilon}{\mathcal{L}^{-1}-\lambda\epsilon}\ . \tag{27}$$

The parameter λ is determined as follows by taking the second moment in Eq. (25):

$$\lambda=\left[\frac{\mu_2(B)}{\tilde{\mu}_2}\right]^{1/2}\ . \tag{28}$$

Here $\mu_2(\alpha)$ is the second moment for $\{t_{ij}(\alpha)\}$. (Note that we only required the change of the *shape* with concentration, but not the change of the *width* of the DOS for $\{\hat{t}_{ij}\}$.) $\tilde{\mu}_2$ in Eq. (28) is the second moment of average DOS for the common band $\{\tilde{t}_{ij}\}$, and is obtained as follows (see the Appendix):

$$\tilde{\mu}_2=\{c_A[\mu_2(A)]^{1/2}+c_B[\mu_2(B)]^{1/2}\}^2\ . \tag{29}$$

We have calculated the DOS for amorphous $Cu_{35}Zr_{65}$ within the SSA to test the quantitative aspect of our theory.

The input DOS for amorphous Cu was prepared by scaling the DOS (Ref. 32) for amorphous Fe with the ratio W(fcc Cu)/W(fcc Fe) = 0.275/0.486 (Ref. 33). (See Fig. 3.) We have calculated the DOS for amorphous Zr as shown in Fig. 3 using the first-principles tight-binding LMTO recursion method.[10] The amorphous structure was generated by using the relaxed DRPHS model with 1500 Zr atoms and truncated Morse pair potentials. The d electron number $N_{Zr}=2.5$ was taken from the d component of our first-principles calculations, and $N_{Cu}=9.4$ was chosen so that the position of the Cu peak in the DOS is in agreement with that in the UPS data by Oelhafen *et al.*[34]

Calculated results are presented in Figs. 4 and 5 together with the recent result obtained by Fujiwara[10] and

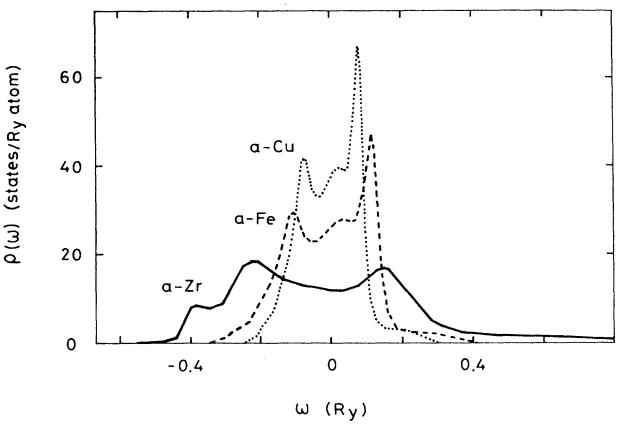

FIG. 3. Input densities of states (DOS's) for amorphous Cu (dotted curve), Fe (dashed curve) (Ref. 32), and Zr (solid curve) pure metals. The DOS for Cu was obtained by scaling that of amorphous Fe with the ratio 0.275/0.486 (Ref. 33), and that for Zr was calculated by means of the tight-binding LMTO recursion method.

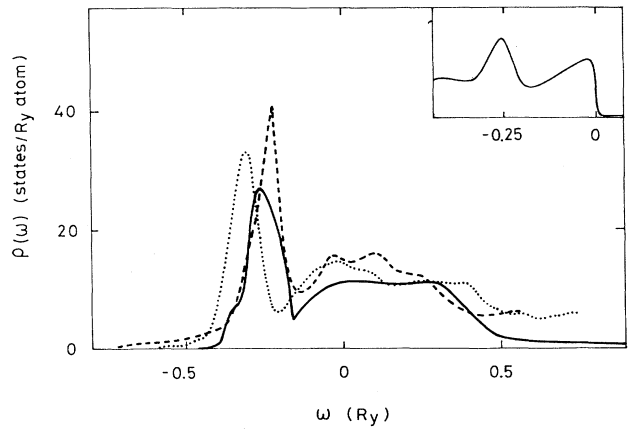

FIG. 4. The DOS for amorphous $Cu_{35}Zr_{65}$ alloys obtained by means of the single-site theory with the GM model (solid curve), the tight-binding LMTO recursion method (dashed curve) (Ref. 10), and the orthogonalized LCAO method (dotted curve) (Ref. 12). The inset shows the experimental data of the UPS by Oelhafen *et al.* (Ref. 34).

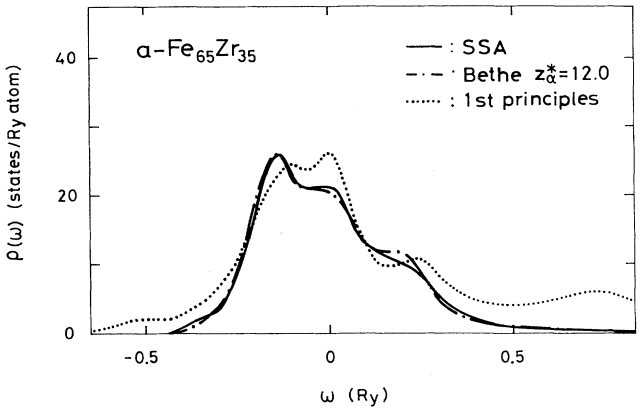

FIG. 6. The DOS for amorphous $Fe_{65}Zr_{35}$ alloys calculated with use of the single-site approximation (solid curve), the Bethe-type approximation with coordination number $z_\alpha^* = 12$ (dot-dashed curve; see Sec. IV), and the tight-binding LMTO recursion method (dotted curve).

that obtained by Ching *et al.*[12] with use of the orthogonalized linear combination of atomic orbital method. In spite of its simplicity, the SSA based on the GM model reproduces an overall structure having a narrow Cu band with a peak and broad Zr band. The DOS's in our theory have less structure as compared with more reliable results because of the single-site approximation and the use of single-band model.

We have also examined the validity of the single-site theory in amorphous $Fe_{90}Zr_{10}$ and $Fe_{65}Zr_{35}$ alloys. Calculated DOS in the amorphous $Fe_{90}Zr_{10}$ alloy was found to agree reasonably with the first-principles results, but a considerable disagreement was found in amorphous $Fe_{65}Zr_{35}$ alloys as shown in Fig. 6, where the parameters $N_{Fe}=7.0$ and $N_{Zr}=3.2$ are chosen from the results of the tight-binding LMTO recursion method at 65 at. % Fe.

The first-principles result shows a shoulder at 0.25 Ry due to the Zr subband and a two-peak structure in the Fe subband. In particular, the peak at higher energy in the Fe subband is located around the Fermi level, which might play an important role in the ferromagnetism of amorphous $Fe_{65}Zr_{35}$ alloys according to the Stoner criterion. The SSA with use of the GM model does not reproduce this peak. This shortcoming remains unimproved, even if we adopt the Bethe approximation going beyond the SSA as long as we fix the coordination number to be 12. We, therefore, improve the theory in the next section.

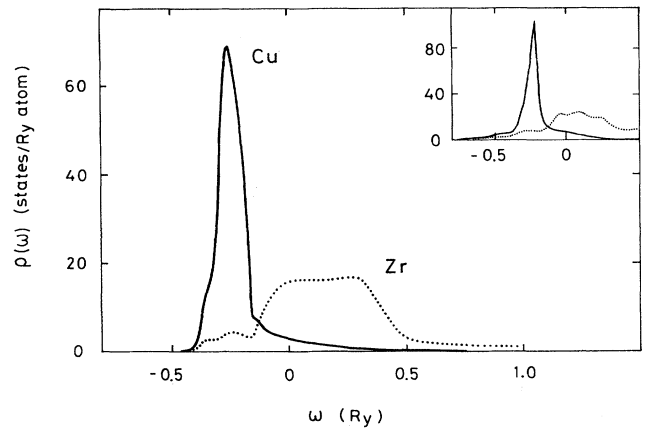

FIG. 5. Local DOS for Cu (solid curve) and Zr (dotted curve) parts in amorphous $Cu_{35}Zr_{65}$ alloys in the single-site theory. The inset shows the first-principles results by Fujiwara (Ref. 10).

IV. BETHE-TYPE APPROXIMATION WITH ATOMIC-SIZE EFFECTS

The amorphous alloys with large atomic-size difference may cause a structural change, which is not obtained by the geometrical mean model. An example is shown in Fig. 7. There, one of the B atoms in the amorphous pure-metal B is replaced by an impurity atom A with larger atomic radius. The nearest-neighbor (NN) shell is expected to expand according to the relation $R_{ij}^{\alpha\gamma}=(R_{ij}^{\alpha\alpha}R_{ij}^{\gamma\gamma})^{1/2}$, so that there is no change in the coordination number on the NN shell. However, more distant atoms may not satisfy such a relation. A few of the B atoms outside the NN shell are expected to fall into the NN shell with the expansion of the NN shell as shown in Fig. 7 by an arrow. This causes the change of the coordination number around the A atom. In what follows, we take into account such a difference in coordination numbers between A and B atoms.

We start from Eq. (3), which does not assume the relation $R_{ij}^{\alpha\gamma}=(R_{ij}^{\alpha\alpha}R_{ij}^{\gamma\gamma})^{1/2}$, and define the Green's function $G'_{ij}=r_\alpha^{(c)}G_{ij}r_\gamma^{(c)*}$ as follows:

$$G'=(L^{-1}-t)^{-1}\ . \tag{30}$$

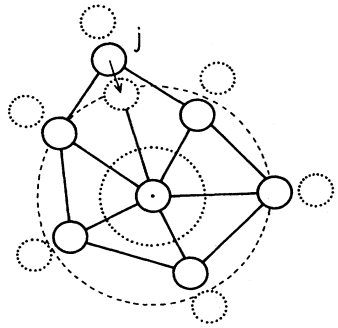

FIG. 7. Schematic rearrangement of neighboring atoms when the A atom with a large atomic size is embedded in amorphous pure B metal with a small size. The surrounding atoms are expected to be expanded according to the GM model, but the B atom on site j outside the shell may approach the A atom at the central site, so that the coordination number around the A atom increases.

Here $(t)_{ij}=t_{ij}$, and the locator L is defined by

$$(L^{-1})_{ij}=|r_\alpha^{(s)}|^2(\hat{L}^{-1})_{ij}=\frac{\omega+i\delta-\epsilon_i}{|r_\alpha^{(c)}|^2}\delta_{ij} . \tag{31}$$

Next we consider a cluster with the NN shell, and make the locator expansion in the Green's function as follows:[31]

$$G'_{00}=L_0+L_0\sum_j t_{0j}G'_{j0} , \tag{32}$$

$$G'_{j0}=L_j t_{j0}G'_{00}+L_j S'_j(L)G'_{j0}+L_j\sum_{i\neq j,0}T_{ji}(L)G'_{i0} . \tag{33}$$

Here we have neglected the transfer integrals between the central atom and the atoms outside the cluster. The self-energy S'_j (T_{ji}) denotes the sum of all the paths, which start from site j and end at site j (i) without returning to the cluster on the way.

In the Bethe approximation, we neglect T_{ji}, which produces the paths with loops between the atoms on the NN shell. Solving Eqs. (32) and (33), we obtain the Green's function $G_{00}=G'_{00}/|r_\alpha^{(c)}|^2$:

$$G_{00}=\frac{1}{|r_\alpha^{(c)}|^2}\left[L_\alpha^{-1}-\sum_{j\neq 0}^{z}\frac{t_{j0}^2}{L_j^{-1}-S'_j(L)}\right]^{-1} . \tag{34}$$

It should be noted that the coordination number z of the central atom α now appears as a random variable in the above equation.

At this stage, we assume the geometrical mean $R_{ij}^{\alpha\gamma}=(R_{ij}^{\alpha\alpha}R_{ij}^{\gamma\gamma})^{1/2}$ for the z atoms on the NN shell. Adopting Eq. (5), we obtain

$$G_{00}=\frac{1}{|r_\alpha|^2}\left[\hat{L}_\alpha^{-1}-\sum_{j\neq 0}^{z}\frac{\hat{t}_{j0}^2}{\hat{L}_j^{-1}-\dfrac{S'_j(L)}{|r_j^{(s)}|^2}}\right]^{-1} . \tag{35}$$

Next we replace the outside of the cluster with the GM model with assumptions (i)–(iv), so that $S'_j(L)/|r_j^{(s)}|^2$ is replaced by $S'_j(\hat{L})$. We then introduce an effective self-energy $\mathcal{S}(\mathcal{L})$ when the configurational as well as structural averages are taken outside the cluster:

$$G_{\alpha\alpha}=\frac{1}{|r_\alpha|^2}\left[\hat{L}_\alpha^{-1}-\sum_{j\neq 0}^{z}\frac{\hat{t}_{j0}^2}{\hat{L}_j^{-1}-\mathcal{S}(\mathcal{L})}\right]^{-1} . \tag{36}$$

The random variables inside the cluster with the central atom α and NN shell are now the number of α atoms on the NN shell n, the coordination number z, and the squares of transfer integrals $\{y_j=\hat{t}_{j0}^2\}$. Introducing the probability $p_\alpha(z)$ of finding z sites on the NN shell of atom α, the probability $p_\alpha(z|n)$ of finding n atoms of type α on the NN shell with z sites, and the probability $p_s(y_j)dy_j$ of finding $\hat{t}_{j0}^2$ between y_j and y_j+dy_j, we obtain the averaged Green's function for the type of atom α as follows:

$$[[G_{\alpha\alpha}]_c]_s=\sum_{z,n}p_\alpha(z)p_\alpha(z|n)\int\left[\prod_j^{z}p_s(y_j)dy_j\right]G_{\alpha\alpha} . \tag{37}$$

The conditional probability $p_\alpha(z|n)$ is given by a binomial distribution function within the pair approximation as follows:

$$\Gamma(n,z,p^{\alpha\alpha})=\frac{z!}{n!(z-n)!}(p^{\alpha\alpha})^n(1-p^{\alpha\alpha})^{z-n} . \tag{38}$$

Here $p^{\alpha\alpha}$ is the probability of finding atom α at the neighboring site of atom α which is assumed to be independent of z. It is given by the atomic short-range order (ASRO) parameter τ_α as follows:

$$p^{\alpha\alpha}=c_\alpha+c_{\bar{\alpha}}\tau_\alpha . \tag{39}$$

Note that τ_A and τ_B are not independent each other because of the following relation for the number of A-B pairs:

$$\tau_{\bar{\alpha}}=1-\frac{z_\alpha^*}{z_{\bar{\alpha}}^*}(1-\tau_\alpha) . \tag{40}$$

Here z_α^* denotes the average coordination number on the NN shell of atom α.

For the distribution $p_\alpha(z)$, we adopt the simplest expression,

$$p_\alpha(z)=(z_\alpha^*-[z_\alpha^*])\delta_{z[z_\alpha^*]+1}+([z_\alpha^*]+1-z_\alpha^*)\delta_{z[z_\alpha^*]} , \tag{41}$$

which satisfies the conditions $1=\sum_z p_\alpha(z)$ and $z_\alpha^*=\sum_z p_\alpha(z)z$. Note that atoms with a larger size are expected to have fewer coordination numbers, so that the difference between z_A^* and z_B^* means that in the atomic size.

Finally, we adopt the decoupling approximation for $p_s(y_j)$, which is correct up to the second moment:

$$\int f(y)p_s(y)dy=\tfrac{1}{2}\sum_{\nu=\pm}f\{[y]_s+\nu[(\delta y)^2]_s^{1/2}\} . \tag{42}$$

Here $f(y)$ is a function of y, and $\delta y\equiv y-[y]_s$. This ap-

proximation has been used in the theory for amorphous pure metals.[35]

By making use of these approximations, the average Green's function (37) is expressed as follows:

$$[[G_{\alpha\alpha}]_c]_s=\sum_z p_\alpha(z)\sum_{n=0}^{z}\Gamma(n,z,p^{\alpha\alpha})\sum_{i=0}^{n}\sum_{j=0}^{z-n}\Gamma(i,n,\tfrac{1}{2})\Gamma(j,z-n,\tfrac{1}{2})G_{\alpha\alpha}(znij)\ , \tag{43}$$

$$G_{\alpha\alpha}(znij)=\frac{1}{|r_\alpha|^2}\left[\hat{L}_\alpha^{-1}-\left[n+(2i-n)\frac{[(\delta y)^2]_s^{1/2}}{[y]_s}\right][y]_sK_\alpha-\left[z-n+(2j-z+n)\frac{[(\delta y)^2]_s^{1/2}}{[y]_s}\right][y]_sK_{\bar{\alpha}}\right]^{-1}\ , \tag{44}$$

$$K_\alpha=(\hat{L}_\alpha^{-1}-\mathcal{S})^{-1}\ . \tag{45}$$

Here the average $[y]_s$ is obtained from the second moment [see Eq. (11)] and an average coordination number z^* as follows:

$$[y]_s=\frac{\mu_2(B)}{z^*}\ . \tag{46}$$

The fluctuation $[(\delta y)^2]_s^{1/2}/[y]_s$ in Eq. (44) is obtained from the relation $\hat{t}_{ij}\propto R_{ij}^{-\kappa}$ [see assumption (iii) in the GM model]:

$$\frac{[(\delta y)^2]_s^{1/2}}{[y]_s}=2\kappa\frac{[(\delta R)^2]_s^{1/2}}{[R]_s}\ , \tag{47}$$

$[R]_s$ $\{[(\delta R)^2]_s^{1/2}\}$ being the average (fluctuation) of the NN interatomic distance in amorphous pure metals.

The self-energy of the GM model $\mathcal{S}$ in Eq. (45) is obtained as follows. First, we express the coherent Green's function of the GM model within the Bethe approximation as

$$[(\mathcal{L}^{-1}-\hat{t})^{-1}]_{00}=\left[\mathcal{L}^{-1}-\sum_{j\neq0}^{z}\frac{\hat{t}_{j0}^2}{\mathcal{L}^{-1}-S_j'(\mathcal{L})}\right]^{-1}\ . \tag{48}$$

Here the effective locator is determined from the CPA equation (22).

When we take the structural average, we replace $S_j'(\mathcal{L})$ with the effective self-energy $\mathcal{S}$. The latter is determined by the self-consistent equation:

$$F(\mathcal{L}^{-1})=\left[\left[\mathcal{L}^{-1}-\sum_{j\neq0}^{z}\frac{\hat{t}_{j0}^2}{\mathcal{L}^{-1}-\mathcal{S}}\right]^{-1}\right]_s\ . \tag{49}$$

To obtain the approximate expression for $\mathcal{S}$, we rewrite Eq. (49) as follows:

$$F(\mathcal{L}^{-1})=[(\mathcal{L}^{-1}-\theta K)^{-1}]_s\ , \tag{50}$$

$$K=(\mathcal{L}^{-1}-\mathcal{S})^{-1}\ . \tag{51}$$

Here $\theta=\sum_{j\neq0}^{z}y_j$, and K is connected with K_α in Eq. (45) via

$$K_\alpha=(\hat{L}_\alpha^{-1}-\mathcal{L}^{-1}+K^{-1})^{-1}\ . \tag{52}$$

It should be noted that the structural disorder in Eq. (50) appears only via the random variable θ. By making use of the decoupling approximation,

$$[(\delta\theta)^{2n+k}]_s\approx[(\delta\theta)^2]_s^n[(\delta\theta)^k]_s\quad(k=0,1)\ ,$$

we obtain

$$F(\mathcal{L}^{-1})=\tfrac{1}{2}\sum_{\nu=\pm}\frac{1}{\mathcal{L}^{-1}-([\theta]_s+\nu[(\delta\theta)^2]_s^{1/2})K)}\ , \tag{53}$$

where $\delta\theta=\theta-[\theta]_s$, and $[\theta]_s=z^*[y]_s=\mu_2(B)$.

Solving Eq. (53), we obtain

$$K=\frac{2F\mathcal{L}^{-1}-1\pm\left[1+4\dfrac{[(\delta y)^2]_s}{z^*[y]_s^2}F\mathcal{L}^{-1}(F\mathcal{L}^{-1}-1)\right]^{1/2}}{2z^*[y]_s\left[1-\dfrac{[(\delta y)^2]_s}{z^*[y]_s^2}\right]F}\ . \tag{54}$$

The sign at the right-hand side should be chosen to be $\mathrm{Im}K<0$. We can calculate $F(\mathcal{L}^{-1})$ from Eq. (21) when the model DOS $[\rho^0(\epsilon)]_s$ for $\{\hat{t}_{ij}\}$ does not depend on the concentration. We can then calculate the electronic structure of amorphous alloys from Eqs. (43), (44), (52) and (54).

When we take into account the concentration dependence of the transfer integrals $\hat{t}$ adopting the common band model defined by Eq. (25), we obtain the explicit expression for K (i.e., $\mathcal{S}$) from the averaged DOS for constituent amorphous metals, $[\rho_A^0(\epsilon)]_s$ and $[\rho_B^0(\epsilon)]_s$ as follows.

The Green's function $F(\mathcal{L}^{-1})=[(\mathcal{L}^{-1}-\lambda\tilde{t})^{-1}]_{00}$ is expressed by a self-energy $\tilde{\mathcal{S}}$ for the transfer integral $\tilde{t}_{ij}$ as follows:

$$F(\mathcal{L}^{-1})=\left[\left[\mathcal{L}^{-1}-\sum_{j\neq0}^{z}\frac{\lambda^2\tilde{t}_{j0}^2}{\mathcal{L}^{-1}-\lambda\tilde{\mathcal{S}}}\right]^{-1}\right]_s\ . \tag{55}$$

Comparing Eq. (55) with Eq. (50), we obtain

$$K=(\mathcal{L}^{-1}-\lambda\tilde{\mathcal{S}})^{-1}\ . \tag{56}$$

Next, we approximate $\tilde{\mathcal{S}}$ by an average of those for amorphous A and B metals.

$$\tilde{\mathcal{S}}=c_A\mathcal{S}(A)+c_B\mathcal{S}(B)\ . \tag{57}$$

The self-energy $\mathcal{S}(\alpha)$ for amorphous pure metal α is defined by the Green function $F_\alpha(\mathcal{L})$ [see Eq. (27)] as follows:

$$F_\alpha(\mathcal{L}^{-1})=\left[\left[\mathcal{L}^{-1}-\sum_{j\neq0}^{z}\frac{\lambda^2t_{j0}(\alpha)^2}{\mathcal{L}^{-1}-\lambda\mathcal{S}(\alpha)}\right]^{-1}\right]_s\ . \tag{58}$$

Solving the above equation in the same way as in Eq. (49), we obtain

$$K_\alpha^0 \equiv [\mathcal{L}^{-1}-\lambda\mathcal{S}(\alpha)]^{-1} = \frac{2F_\alpha\mathcal{L}^{-1}-1\pm\left[1+4\dfrac{[(\delta y)^2]_s}{z^*[y]_s^2}F_\alpha\mathcal{L}^{-1}(F_\alpha\mathcal{L}^{-1}-1)\right]^{1/2}}{2\lambda^2\mu_2(\alpha)\left[1-\dfrac{[(\delta y)^2]_s}{z^*[y]_s^2}\right]F_\alpha} . \quad (59)$$

Here $\mu_2(\alpha)=z^*[t_{j0}(\alpha)^2]_s$, and F_α and λ are given by Eqs. (27) and (28), respectively.

From Eqs. (56), (57), and (59), we obtain an approximate expression of K:

$$K=[c_A(K_A^0)^{-1}+c_B(K_B^0)^{-1}]^{-1} . \quad (60)$$

In the improved theory, we assume the average atomic levels $[[\epsilon_\alpha]_s]_c$ and the effective medium $\mathcal{L}^{-1}(\omega+i\delta)$ (for example, $\sum_\alpha c_\alpha\hat{L}_\alpha^{-1}$), and calculate F_α from Eq. (27), and λ from Eqs. (28) and (29) using the input DOS $[\rho_\alpha^0]_s$. We then obtain K from Eqs. (59) and (60), therefore calculate $F(\mathcal{L}^{-1})$ from Eq. (53). $[[\epsilon_\alpha]_s]_c$ and $\mathcal{L}^{-1}(\omega+i\delta)$ are self-consistently obtained by solving the CPA equation (22) and the charge neutrality condition (23) with $F(\mathcal{L}^{-1})$ defined by Eq. (53). Next we can calculate K_α from Eq. (52), and $G_{\alpha\alpha}(znij)$ from Eq. (44). The atomic levels $\{\epsilon_\alpha(znij)\}$ in the locator $\hat{L}_\alpha^{-1}$ of $G_{\alpha\alpha}(znij)$ are determined again from the charge neutrality condition in each configuration.

$$n_\alpha=\int_{-\infty}^{0}d\omega\left[-\frac{D}{\pi}\right]\mathrm{Im}G_{\alpha\alpha}(znij) . \quad (61)$$

Finally, the averaged DOS is obtained from Eq. (24) with Eq. (43).

The input parameters are electron number n_α, the DOS $[\rho_\alpha^0(\epsilon)]_s$, the fluctuation of the interatomic distance $[(\delta R)^2]_s^{1/2}/[R]_s$, the exponent κ [see Eq. (47)], the average coordination numbers z^* and z_α^*, and the ASRO parameter τ_A (or τ_B). We choose $z^*=12$ in the following numerical calculations. The LEE's are described by $[(\delta R)^2]_s^{1/2}/[R]_s$, $\{z_\alpha^*\}$, and $\{\tau_\alpha\}$. In particular, the coordination numbers $\{z_\alpha^*\}$ are the new variables characteristic to amorphous alloys.

The present theory reduces to the Bethe theory, which has recently been proposed by one of the authors,[35] in the limit of amorphous pure metal, and essentially reduces to the Bethe theory of LEE's proposed by Miwa [31] and Brouer *et al.*[36] in the case of substitutional alloys with the same band width. In the case of amorphous alloys, the present theory describes the LEE's caused by $2\times2^{z^*}\times2^{z^*}$ ($\sim10^7$) of atomic and structural configurations on the NN shell, in particular, describe the effects of the difference in atomic size in amorphous alloys via the coordination number $\{z_\alpha^*\}$.

V. ATOMIC-SIZE EFFECTS AND ASRO EFFECTS IN AMORPHOUS Fe-Zr and Co-Y ALLOYS

We have calculated the DOS in amorphous $Fe_{65}Zr_{35}$ using the improved Bethe theory to examine the validity of the theory and the effects of the atomic-size difference. The results are presented in Fig. 8. We chose there the coordination number $z_{Zr}^*=14.0$ so as to reproduce the shoulder at 0.25 Ry, and varied z_{Fe}^* from 12 to 8 fixing the ASRO $\tau_{Fe}=0.0$ and $[(\delta R)]_s^{1/2}/[R]_s=0.06$ (Ref. 26) to examine the effects of the atomic-size difference on the Fe local DOS via the coordination number.

Calculated DOS's generally show a two-peak structure below the Fermi level. The amplitude of the low-energy peak is larger than that of the high-energy one when $z_{Fe}^*=12$. With decreasing z_{Fe}^*, the high-energy peak rapidly develops and becomes dominant at $z_{Fe}^*\approx8.0$. It is seen that the first-principles DOS's calculated by the tight-binding LMTO recursion method is semiquantitatively reproduced by means of the improved theory with $z_{Fe}^*\approx9.0$.

The amorphous $Fe_{65}Zr_{35}$ alloy is known to show the ferromagnetism with the ground-state magnetization $0.95\mu_B$.[37,38] The high DOS at the Fermi level is important for the appearance of the ferromagnetism according to the Stoner criterion. The present results suggest that the ferromagnetism in amorphous $Fe_{65}Zr_{35}$ alloys originates in the formation of the high-energy peak due to the atomic-size difference. It should be noted that the effect is characteristic of amorphous metallic alloys and is not seen in the simple substitutional alloys.

The theory describes the effects of ASRO $\{\tau_\alpha\}$. We show the DOS for amorphous $Fe_{65}Zr_{35}$ alloys with

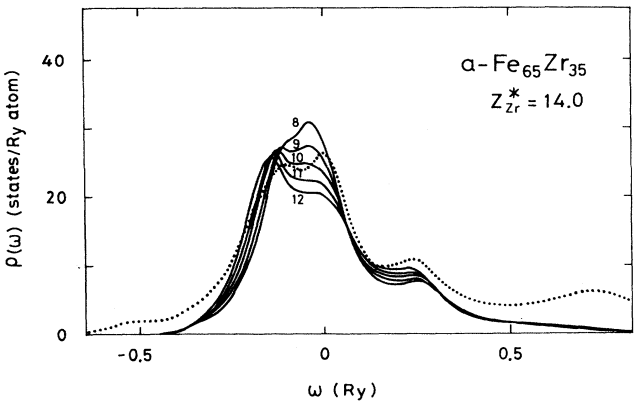

FIG. 8. The calculated DOS for amorphous $Fe_{65}Zr_{35}$ alloys with use of the Bethe-type approximation (solid curve) and the tight-binding LMTO recursion method (dotted curve). The numbers for the solid curves denote the average coordination numbers of Fe atoms (z_{Fe}^*).

$\tau_{Fe}=\pm 0.3$ in Fig. 9 as an example. It is seen that the width of the Fe subbands shrinks, and the shoulder around $\omega=0.2$ Ry increases with decreasing τ_{Fe} because such a change of τ_α decreases the number of Fe-Fe pairs, and increases the mixing between Fe $3d$ and Zr $4d$ orbitals. In particular, the DOS's at the Fermi level increase with increasing Fe-Fe pairs.

Recently, Krebs *et al.*[38] investigated the amorphous Fe_cZr_{1-c} $(0.2\leq c\leq 0.9)$ alloys. They found that annealed amorphous $Fe_{50}Zr_{50}$ alloys tend to separate into amorphous $Fe_{62}Zr_{38}$ and $Fe_{33}Zr_{67}$ alloys, so that the alloys show the ferromagnetism with the ground-state magnetization of about $0.5\mu_B$, although the magnetization of unannealed ones mostly disappears. This phenomenon might be explained by the increase of the DOS at the Fermi level with increasing Fe-Fe pairs as we have shown in Fig. 9.

Another example which exhibits the atomic-size effects on the stability of ferromagnetism is the amorphous Co_2Y alloy. This alloy shows the ferromagnetism with the ground-state magnetization $1.0\mu_B$,[39–41] although the crystalline counterpart shows the paramagnetism.[42] Inoue and Shimizu[13] calculated the DOS for amorphous and crystalline Co_2Y alloys using a tight-binding recursion method and found that the ferromagnetism in amorphous Co_2Y is stabilized by the formation of a peak around the Fermi level. (See the inset of Fig. 10.)

We performed the same calculations as in the amorphous $Fe_{65}Zr_{35}$ alloy to examine the atomic-size effects via the coordination numbers. The parameters were chosen to be $n_{Co}=8.0$, $n_Y=1.7$, $\tau_{Co}=0.0$, and $[(\delta R)^2]_s^{1/2}/[R]_s=0.06$. The input DOS $[\rho_\alpha(\epsilon)]_s$ are taken from those of amorphous Fe and Zr after scaling the bandwidth with the ratios 0.441/0.393 (Ref. 33) and 0.463/0.544 (Ref. 33), respectively.

Calculated results again indicate the development of high-energy peak with decreasing z^*_{Co} as shown in Fig. 10. This implies that the ferromagnetism in amorphous Co_2Y alloy is caused by an averaged coordination number z^*_{Co} (≈ 9.0) smaller than z^*_{Zr} because of the atomic-size difference.

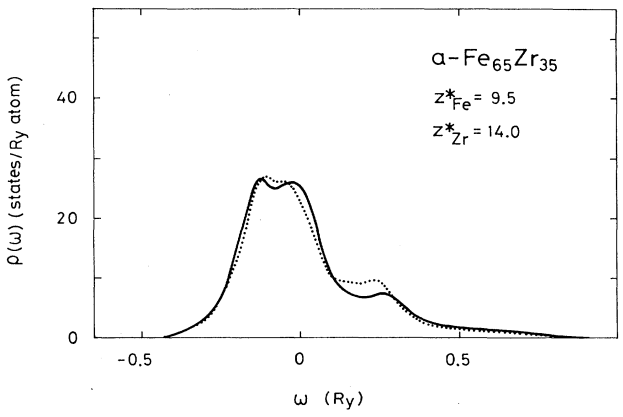

FIG. 9. The calculated DOS with atomic short-range order $\tau_{Fe}=-0.3$ (dotted curve) and $\tau_{Fe}=0.3$ (solid curve) in amorphous $Fe_{65}Zr_{35}$ alloys.

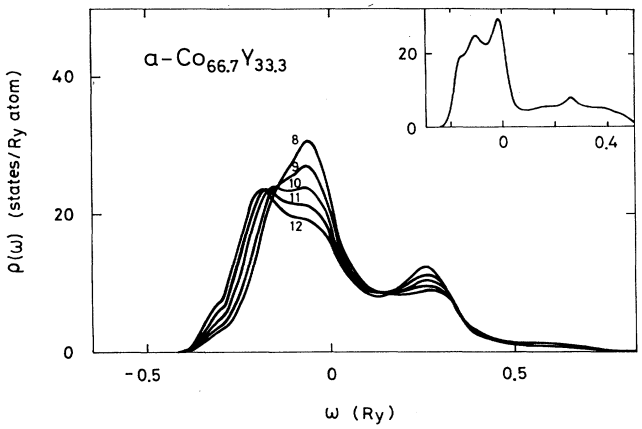

FIG. 10. Calculated DOS for amorphous Co_2Y alloys with various average coordination numbers of Co ($z^*_{Co}=8$–12). z^*_Y is fixed to be 12. The inset shows the result calculated by Inoue and Shimizu (Ref. 13).

VI. SUMMARY

In the present paper, we have proposed the GM model for the amorphous structure and transfer integrals. The model transforms the off-diagonal configurational disorder into a diagonal disorder in a tight-binding Hamiltonian, which makes the theoretical treatment much simpler. We have developed a Bethe-type theory as well as a single-site theory for the electronic-structure calculations in amorphous alloys on the basis of the GM model. The theory drastically simplifies the numerical calculations of electronic structures; the DOS of amorphous alloys are calculated at any concentration from the data for constituent amorphous pure metals ($[\rho_\alpha(\epsilon)]_s$ and $[(\delta R)]_s^{1/2}/[R]_s$) and a few local parameters such as z^*_α and τ_α.

By comparing our results with those based on the tight-binding LMTO recursion method, we have demonstrated that the Bethe-type theory describes semiquantitatively the electronic structures of amorphous transition-metal alloys with a suitable choice of local parameters, in spite of a simple model Hamiltonian and the GM model.

The theory describes the LEE's characterized by z^*_α and τ_α. The LEE's dominate the local bandwidth and the shape of the DOS. In fact, we have demonstrated that the difference in the coordination numbers of constituent atoms with the different atomic sizes is indispensable for the stability of ferromagnetism in amorphous $Fe_{65}Zr_{35}$ and Co_2Y alloys. Furthermore, we pointed out that the enhancement of the Fe DOS at the Fermi level with increasing ASRO parameter τ_{Fe} is consistent with the appearance of ferromagnetism in annealed $Fe_{50}Zr_{50}$ amorphous alloys. More detailed investigations concerning the problems in the structure vs magnetism will be published elsewhere.

One of the possible applications of the present theory is the calculations of finite-temperature magnetic properties in amorphous transition-metals alloys. We have recently proposed a finite-temperature theory of amorphous metallic magnetism on the basis of the functional integral method,[35] and have clarified a variety of magnetism in amorphous transition metals.[43] In this theory, one needs the Green's functions of a one-electron system with random exchange fields. The present approach allows us to calculate such Green's functions in amorphous alloys. This means that we can investigate the magnetism in amorphous alloys at finite temperatures by combining the present theory with the finite-temperature theory of magnetism.

The application of the present approach to the amorphous rare-earth transition-metal alloys also seems to be possible. In this case, one has to take into account the localized f electrons with use of a suitable model Hamiltonian. The effects of the structural and configurational disorders on the transition-metal $3d$ and rare-earth $5d$ band electrons as described by Eq. (1) are still expected to be important in the alloys. We hope that the present approach will play an important role in qualitative or semiquantitative understanding of magnetism in these amorphous metallic systems.

ACKNOWLEDGMENTS

One of the authors (Y.K.) would like to thank Dr. R. L. Jacobs for valuable discussions at Imperial College. This work was partly supported by the Grant-in-Aid for Scientific Research from the Ministry of Education, Science, and Culture in Japan.

APPENDIX A: DERIVATION OF EQ. (3.16)

The second moment for the common band $\{\hat{t}_{ij}\}$ is expanded as follows:

$$\tilde{\mu}_2 = c_A^2 \left[\sum_j t_{j0}(A)^2 \right]_s + 2c_A c_B \left[\sum_j t_{j0}(A) t_{j0}(B) \right]_s + c_B^2 \left[\sum_j t_{j0}(B)^2 \right]_s . \tag{A1}$$

According to the GM model, we have a relation

$$t_{ij}(A) = (r'_A)^2 t_{ij}(B) . \tag{A2}$$

Here r'_A is a site-independent constant and is obtained from the second moments $\mu_2(\alpha) = [\sum_j t_{j0}(\alpha)^2]_s$ as follows:

$$(r'_A)^2 = \left[\frac{\left[\sum_j t_{j0}(A)^2 \right]_s}{\left[\sum_j t_{j0}(B)^2 \right]_s} \right]^{1/2} . \tag{A3}$$

By making use of Eqs. (A2) and (A3), we can rewrite the second term at the right-hand side of Eq. (A1) as follows:

$$\left[\sum_j t_{j0}(A) t_{j0}(B) \right]_s = (r'_A)^2 \left[\sum_j t_{j0}(B)^2 \right]_s = \left[\sum_j t_{j0}(A)^2 \right]_s^{1/2} \left[\sum_j t_{j0}(B)^2 \right]_s^{1/2} . \tag{A4}$$

Substituting Eq. (A4) into Eq. (A1), we obtain the final result [Eq. (29)].

$$\tilde{\mu}_2 = \{ c_A [\mu_2(A)]^{1/2} + c_B [\mu_2(B)]^{1/2} \}^2 . \tag{A5}$$

[1] H. Hiroyoshi and K. Fukamichi, Phys. Lett. **85A**, 242 (1981); J. Appl. Phys. **53**, 2226 (1982).

[2] N. Saito, H. Hiroyoshi, K. Fukamichi, and Y. Nakagawa, J. Phys. F **16**, 911 (1986).

[3] J. M. D. Coey, D. H. Ryan, and R. Buder, Phys. Rev. Lett. **26**, 385 (1987); D. H. Ryan, J. M. D. Coey, E. Batalla, Z. Altounian, and J. O. Ström-Olsen, Phys. Rev. B **35**, 8630 (1987).

[4] K. Fukamichi, T. Goto, H. Komatsu, and H. Wakabayashi, *Proceedings of the 4th International Conference on the Physics of Magnetic Material, City,* edited by W. Gorkowski, H. K. Lachowics, and H. Szymczak (World Scientific, Singapore, 1989) p. 354.

[5] K. Fukamichi, T. Goto, and U. Mizutani, IEEE Trans. Mag. **MAG-23**, 3590 (1987).

[6] L. Krusin-Elbaum, A. P. Malozemoff, and R. C. Taylor, Phys. Rev. B **27**, 562 (1983).

[7] L. M. Roth, Phys. Rev. B **9**, 2476 (1974).

[8] S. Asano and F. Yonezawa, J. Phys. F **10**, 75 (1980).

[9] S. Frota-Pessôa, Phys. Rev. B **28**, 3753 (1983).

[10] T. Fujiwara, J. Non-Cryst. Solids, **61&62**, 1039 (1984).

[11] W. Y. Ching, L. W. Song, and S. S. Jaswal, Phys. Rev. B **30**, 544 (1984).

[12] W. Y. Ching, G. L. Zhao, and Y. He, Phys. Rev. B **42**, 10 878 (1990).

[13] J. Inoue and M. Shimizu, J. Phys. F **15**, 1525 (1985).

[14] J. P. Xanthakis, R. L. Jacobs, and E. Babić, J. Phys. F **16**, 323 (1986).

[15] S. Krompiewski, U. Krauss, U. Krey, Phys. Rev. B **39**, 2819 (1989); U. Krey, S. Krompiewski, and U. Krauss, J. Magn. Magn. Mater. **86**, 85 (1990); **103**, 37 (1992).

[16] H. J. Nowak, O. K. Andersen, T. Fujiwara, O. Jepsen, and P. Vargas, Phys. Rev. B **44**, 3577 (1991).

[17] H. Tanaka and S. Takayama, J. Appl. Phys. **70**, 6577 (1991).

[18] I. Turek, J. Hafner, and Ch. Hausleintner J. Magn. Magn. Mater. **109**, L145 (1992); J. Hafner, Ch. Hausleintner, W. Jank, and I. Turek, J. Non-Cryst. Solids (to be published).

[19] O. K. Andersen, O. Jepsen, and D. Glötzel, in *Highlights of Condensed Matter Theory,* edited by F. Bassani, F. Fumi, and M. P. Tosi (North-Holland, New York, 1985).

[20] R. Haydack, V. Heine, and M. J. Kelly, J. Phys. C **8**, 2591 (1975); V. Heine, Solid State Phys. **35**, 1 (1980).

[21] M. Cyrot, J. Phys. (Paris) **33**, 25 (1972).

[22] J. Hubbard, Phys. Rev. B **19**, 2626 (1979); **20**, 4584 (1979); **23**, 597 (1981).

[23] H. Hasegawa, J. Phys. Soc. Jpn. **46**, 1504 (1979); **49**, 178 (1980).

[24] Y. Kakehashi, Phys. Rev. B **34**, 3243 (1986).

[25] H. Shiba, Prog. Theor. Phys. **46**, 77 (1971).

[26] M. Matsuura, H. Wakabayashi, T. Goto, H. Komatsu, and K. Fukamichi, J. Phys. Condens. Matter **1**, 2077 (1989).

[27] H. S. Chien and Y. Waseda, Phys. Status Solidi A **51**, 593 (1979).

[28] V. Heine, Phys. Rev. **153**, 673 (1967); H. L. Skriver, *The LMTO Method* (Springer-Verlag, Berlin, 1984).

[29]G. S. Cargill, Solid State Phys. **30**, 227 (1975).
[30]Y. Waseda, *The Structure of Non-Crystalline Materials* (McGraw-Hill, New York, 1980).
[31]H. Miwa, Prog. Theor. Phys. **52**, 1 (1974).
[32]T. Fujiwara, Nippon Butsuri Gakkaishi **40**, 209 (1985).
[33]V. L. Moruzzi, J. F. Janak, and A. R. Williams, *Calculated Electronic Properties of Metals* (Pergamon, New York, 1978).
[34]P. Oelhafen, E. Hansen, H. J. Güntherodt, and K. H. Bennemann, Phys. Rev. Lett. **43**, 1134 (1979).
[35]Y. Kakehashi, Phys. Rev. B **41**, 9207 (1990).
[36]F. Brouer, F. Ducastelle, F. Gautier, and J. Van der Rest, J. Phys. F **3**, 2120 (1973).
[37]T. Stobiecki, G. Bayreuther, and H. Hoffmann, in *Proceedings of the Symposium on Magnetic Properties of Amorphous Metals, Benalmadena, 1987,* edited by A. Hernando *et al.* (North-Holland, Amsterdam, 1987).
[38]H. U. Krebs, W. Biegel, A. Bienenstook, D. J. Webb, and T. H. Geballe, Mater. Sci. Eng. **97**, 163 (1988).
[39]K. H. J. Buschow, M. Brouha, J. W. M. Biesterbos and A. G. Dirks, Physica B **91**, 261 (1977).
[40]N. Heiman and N. Kazama, Phys. Rev. B **17**, 2215 (1978).
[41]D. Gignoux, D. Givord, and A. Liénard, J. Appl. Phys. **53**, 2321 (1982).
[42]S. Asano and S. Ishida, J. Phys. F **18**, 501 (1988).
[43]Y. Kakehashi, Phys. Rev. B **43**, 10 820 (1991).